Materials and Design 90 (2016) 60–65

Contents lists available at ScienceDirect

Materials and Design

journal homepage: www.elsevier.com/locate/jmad

Fracture behavior of sandwich-structured metal/amorphous alloy/metal composites

H.F. Tan [a,b], B. Zhang [a,*], Y.K. Yang [b], X.F. Zhu [b], G.P. Zhang [b,*]

[a] Key Laboratory for Anisotropy and Texture of Materials, Ministry of Education, Northeastern University, 3-11 Wenhua Road, Shenyang 110819, PR China
[b] Shenyang National Laboratory for Materials Science, Institute of Metal Research, Chinese Academy of Sciences, 72 Wenhua Road, Shenyang 110016, PR China

ARTICLE INFO

Article history:
Received 1 July 2015
Accepted 19 October 2015
Available online 20 October 2015

Keywords:
Ultrafine grain
Amorphous alloy
Laminated composite
Shear band
Strength, fracture

ABSTRACT

The sandwich-structured ultrafine grained (UFG) Ni/$Fe_{78}B_{13}Si_9$ amorphous alloy/UFG Ni composite were prepared through the electrodeposition technique. Tensile testing of the sandwich composites was conducted and fracture behavior of the composites was characterized. The results show that the yield and ultimate tensile strengths decrease gradually, while the ductility of the sandwich composite increases with increasing UFG-Ni layer thickness. The fracture mode of the sandwich-structured composite varies with changing the constraint UFG-Ni layer thickness. The local necking of the UFG-Ni layers plays an important role in fracture mode of the sandwich composites. The coupling effect of the UFG-Ni layer and amorphous layer on mechanical performance of the sandwich composites is discussed.

1. Introduction

Amorphous alloy is an attractive material with disordered structures, which has given rise to great attention due to its some excellent properties and potential applications [1–8]. The amorphous alloy can have high strength, but the plasticity of the alloy is remarkably poor and the plastic strain is almost close to zero under uniaxial tensile loading [9, 10]. Such low plasticity is attributed to preferential formation of shear bands (SBs) [11–14], which leads to rapid fracture without any plasticity [1,14–18]. Generally, there are two ways, which are expected to enhance ductility of amorphous alloys. One is the promotion of multiplication of SBs because each SB contributes to the plasticity and none carries enough deformation to cause catastrophic failure [19]. The other is the suppression on SBs through reinforced phases and/or structures in the amorphous alloy [20–27]. Obviously, it is necessary to further understand how the SBs can be suppressed or constrained by additionally-introduced phases and/or structures in order to improve the ductility of amorphous alloys.

Laminated composites consisting of two or more constituent layers are expected to have excellent mechanical properties through a proper combination of the properties of the constituent layers [28]. Therefore, a lot of efforts to develop new laminated composites have been conducted for recent years, such as metallic multilayers [28,29], metallic laminated composites [30–33], metal/amorphous alloy laminated composites [34–36], and even bio-inspired nanolayered composites [37–40]. For metal/amorphous alloy laminated composites, Li et al. [34,35] have ever electrodeposited nano-Ni layers on the $Fe_{78}Si_9B_{13}$ amorphous alloy ribbon, and then investigated ductility of the nano-Ni/amorphous alloy laminated composite. They found that the 50 μm-thick nano-Ni layers deposited to the amorphous alloy ribbon could effectively improve the elongation of the amorphous alloy ribbon and that in the laminated composite [34]. In such laminated composite system, a key point is how to understand the coupling effect of constituent layers on the variation of mechanical performance of the laminated composite.

In this paper, ultrafine-grained (UFG)-Ni layers with difference thicknesses were electrodeposited onto Fe-based amorphous alloy ribbons to produce sandwich-structured UFG-Ni/amorphous composites. Mechanical properties of the sandwich-structured composites were investigated by tensile testing at room temperature. Variation of deformation and fracture behaviors of the constituent layers in the composite with the UFG-Ni layer thickness is characterized carefully, and the constraint effects of UFG-Ni layers on fracture behavior of the amorphous layer were analyzed.

2. Experimental

2.1. Preparation of materials

In this study, typical $Fe_{78}B_{13}Si_9$ (at %) (Metglas 2605 S2) metallic glassy ribbons with a thickness of 24 μm, which were prepared by a standard melt spinning technique, were selected. The amorphous ribbons were cut into sheets with dimensions of 40×30 mm^2, and then cleaned ultrasonically in acetone before electrodeposition. UFG-Ni layers with different thicknesses were electrodeposited to the amorphous ribbon by

* Corresponding authors.
E-mail addresses: zhangb@atm.neu.edu.cn (B. Zhang), gpzhang@imr.ac.cn (G. P. Zhang).

http://dx.doi.org/10.1016/j.matdes.2015.10.107
0264-1275/

controlling the deposition time under the same deposition currents in the electrolyte solution composed of 100 g/L $NiSO_4 \cdot 6H_2O$, 50 g/L $NiCl_2 \cdot 6H_2O$, 40 g/L H_3BO_3, 0.1 g/L Sodium Dodecyl Sulfate (SDS) in deionized water [30]. The UFG-Ni layer thickness (t_{Ni}) varies from 3 μm to 30 μm, thus the total thickness of the laminated composite is in a range from 30 to 84 μm.

2.2. Tensile testing and microstructure characterization

Dog-bone shape tensile specimens were prepared by an electro-discharge machine. Gauge dimensions of the tensile specimens are 4 mm in length and 2 mm in width. Uniaxial tensile tests were performed on a testing machine (Instron® E1000 Microtester) at room temperature under a strain rate of 5×10^{-4} s^{-1}. The electric resistance of the composites was monitored by the digital multimeters (Agilent 34410 A). The cross-section morphologies and fracture surfaces of the sandwich composites were examined using laser scanning confocal microscope (LSCM, OLS4000) and scanning electron microscope (SEM, LEO Supra 35). The grain size of the UGF Ni layers was characterized by a transmission electron microscope (TEM, Tecnai G2 F20).

3. Results and discussion

3.1. Microstructures

Fig. 1(a) presents a TEM plan-view image of the Ni layers electrodeposited on two sides of the amorphous ribbon. The corresponding statistic distribution of the grain size reveals that the mean grain size of the Ni layers (see Fig. 1(b)) is 150 ± 40 nm, indicating that the Ni layer has an UFG structure. A TEM image with the corresponding selected-area electron diffraction pattern of the FeSiB amorphous alloy (Fig. 1(c)) indicates that no crystallites appear in the amorphous layer.

3.2. Tensile properties

In order to compare mechanical properties of the composites with the constituent layers, tensile tests of individual 12 μm-thick amorphous ribbons and 50 μm-thick UFG Ni sheets were also conducted in the same conditions. Fig. 2(a) presents tensile engineering stress–strain curves of all the samples. It is clear that all curves of the sandwich samples locate between that of the individual amorphous ribbons and the UFG-Ni sheets. Both the yield strength ($\sigma_{0.2}$) and ultimate tensile strength (σ_{UTS}) decrease gradually (see Fig. 2(b)), while the uniform elongation (ε_{UE}) and the elongation to fracture (ε_f) increase (see Fig. 2(c)) with increasing t_{Ni}. It is worth noting that the strength and ductility of the $t_{Ni} = 3$ μm sample is not improved. Fig. 2(d) shows the relationship between $\sigma_{0.2}$ and ε_{UE} of the samples. The typical trade-off of strength and ductility can be found for the sandwich-structured composites.

3.3. Fracture behavior

Fig. 3(a) shows a LSCM image of the fracture surface of the $t_{Ni} =$ 3 μm sample. Furthermore, a three-dimensional (3D) image (Fig. 3(b)) and the corresponding line scanning of the fracture surface (Fig. 3(c)) reveal that the fracture surface of the amorphous layer is rough but lack of evident SB steps, while both of the UFG-Ni layers exhibit local necking behavior, as shown in Fig. 3(c). This observation indicates that the amorphous layer constrained by both sides of UFG-Ni layers did not fracture in the conventional shear mode along SBs but in the normal fracture mode. Comparatively, Fig. 4(a) presents a LSCM image of the fracture surface of the $t_{Ni} = 20$ μm sample. A 3D LSCM image and the corresponding line scanning profile of the fracture surface are shown in Fig. 4(b) and (c), which show that the amorphous layer fractured in the shear mode through the formation and propagation of SBs, while the UFG-Ni layer in the right side broken in the necking mode. In general, the amorphous layer in the $t_{Ni} = 3$ μm sandwich sample fractured in normal mode, while that in the $t_{Ni} > 10$ μm sandwich samples fractured in shear mode.

For the amorphous layer, a fracture angle (θ_s) relative to the loading direction defined in Fig. 4(c) was characterized based on the line scanning morphologies of the amorphous layers and was presented in Fig. 5 as a function of the UFG-Ni layer thickness. It can be seen that θ_s of the individual amorphous ribbon is 54.5 ± 4.9° measured, which is similar to the extensive observations [15,41]. θ_s becomes larger when t_{Ni} is close to 3 μm due to the normal fracture mode, while θ_s tends to decrease because of the shear fracture mode when $t_{Ni} > 10$ μm.

The variation of θ_s is likely to be associated with the fracture mode and the interface cohesive strength. To estimate the interface cohesion properties between the UFG-Ni and the amorphous layers, the width of interface delamination after tensile fracture of the samples was measured through cross-section observations. Fig. 6 shows that the interface debonding width evidently increases with increasing the UFG-Ni layer

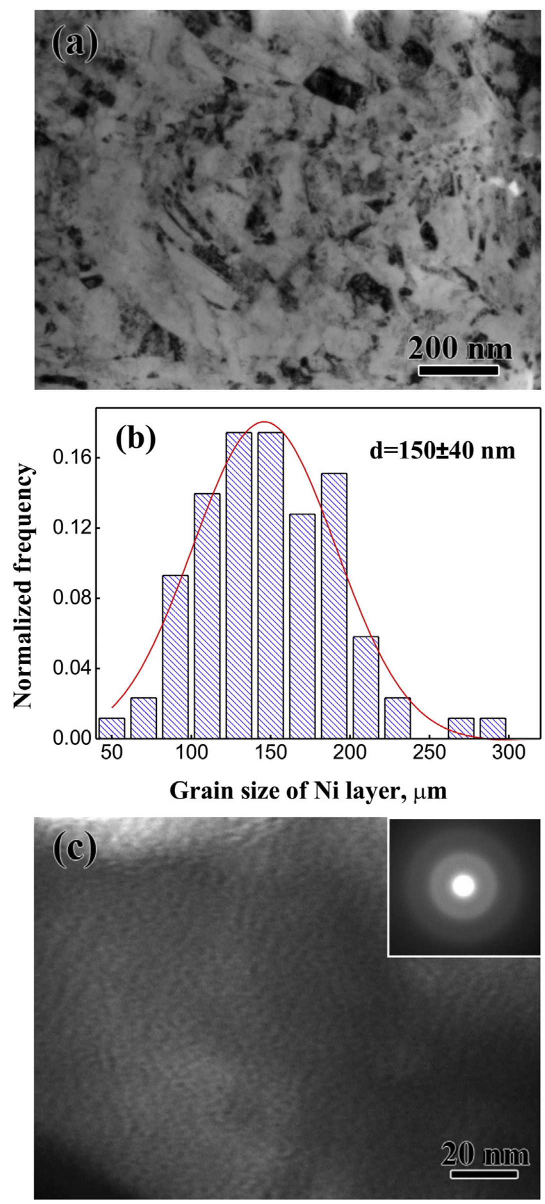

Fig. 1. Microstructure characterization of sandwich-structured UFG-Ni/$Fe_{78}B_{13}Si_9$ amorphous alloy/UFG-Ni composite, (a) TEM cross-sectional image of UFG-Ni layer; (b) distribution of grain size of UFG-Ni layer, (c) TEM image of Fe-based amorphous ribbon.